Enhancement of Phase Sensitivity by Exploring Slow Light in Photonic Crystals

Marin Soljačić[(*)], Steven G. Johnson[(*)], Shanhui Fan[(&)], Mihai Ibanescu[(*)], Erich Ippen[(*)], and J.D. Joannopoulos[(*)]

[(*)] Department of Physics, and Center for Materials Science and Engineering, Massachusetts Institute of Technology, Cambridge, MA 02139

[(&)] Department of Electrical Engineering, Stanford University, Stanford, CA 94305

We demonstrate how dramatic increases in the induced phase shifts caused by small changes in the index of refraction can be achieved by using very slow group velocities of light, which are readily achievable in photonic crystal systems. Combined with the fact that small group velocity greatly decreases the power requirements needed to operate a device, enhanced phase sensitivity may be used to decrease the size and power requirements of many devices, including switches, routers, all-optical logical gates, wavelength converters, etc. We demonstrate how these advantages can be used to design switches smaller than 20*200 square microns in size, using readily available materials, and at modest levels of power. With this approach, one could have $\sim 10^5$ such devices on a surface 2*2 square cm, making it an important step towards large-scale all-optical integration.

The size of high-speed active elements is presently a critical problem in the path toward large scale optical integration. The smallest all-optical and electro-optical switches are on the order of millimeters [1,2,3], with little promise of getting much smaller. The reason for this is that the changes in index of refraction induced by electro-optical or non-linear optical effects, which are used to operate the devices, are very small (δn is $\mathcal{O}(0.001)$). If one wants to use an induced δn to shift the phase of signal by π[(*)] after propagating through length L of some material, the induced phase change is then $\pi = 2\pi L \delta n / \lambda_{AIR} \Rightarrow L = \lambda_{AIR}/2\delta n$, requiring the size of the device to be millimeters or more.

It is well known that non-linear effects can be enhanced in systems with slow group velocity, due to the compression of the local energy density. Our observation in this article [4] is that the sensitivity of the phase to the induced change in the index of refraction can be drastically enhanced if one operates in the regimes of slow group velocities. Slow group velocities occur quite commonly in photonic crystals, systems with electro-magnetically induced transparency [5,6,7,8] etc. According to perturbation theory, the induced shift in the optical frequency of a photonic band mode at a fixed k, due to a small δn is given by: $\delta\omega(k)/\omega = -\sigma * \delta n/n$, where σ specifies the fraction of the total energy of the mode in question that is stored in the region where δn is being applied. However, since the induced phase shift actually depends on δk, the phase shift can be greatly enhanced if $v_G = d\omega/dk$ is small, as illustrated in Figure 1. To make this more precise, the induced phase shift is $\delta\phi = L*\delta k \approx L*\delta\omega/(d\omega/dk) \Rightarrow \delta\phi \approx -L\omega\sigma\delta n/(nv_G)$. In other words, if $\delta\phi = -\pi$:

[*] A phase change of π can be used to switch the signal on-off by placing the material in an interferometer. For example, one could use a Mach-Zehnder interferometer which we describe below.

Active and Passive Optical Components for WDM Communications II, Achyut Kumar Dutta, Abdul Ahad Sami Awwal, Niloy K. Dutta, Katsunari Okamoto, Editors, Proceedings of SPIE Vol.4870 (2002) © 2002 SPIE · issn

$$\frac{L}{\lambda_{AIR}} \approx \frac{1}{2\sigma}\left(\frac{n}{\delta n}\right)\left(\frac{v_G}{c}\right), \qquad (1)$$

or for a given δn the size of the device scales linearly with v_G.

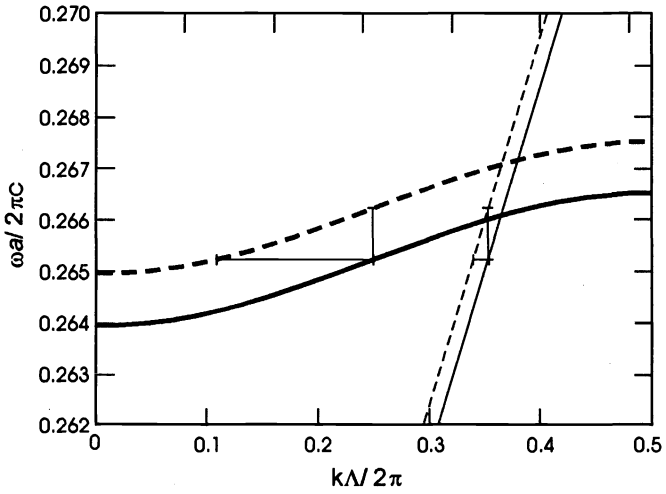

Figure 1: The induced change in the photonic band frequency in a material depends mostly on the induced index of refraction change. However, depending on the local group velocity, this can lead to drastically different changes in the wave-vector. Here we show this effect for two dispersion curves: the slow-light band with v_G=0.022c used in a device proposed in this article (thick line), and the dispersion curve of a uniform material with n=3.5 (thin line). We apply the same frequency shift ($\delta\omega$=0.001) to both of these dispersion curves, to get the respective dashed curves. As we see, the same $\delta\omega$ leads to two very different δk's.

An electro-optical device that is smaller in length by a factor of v_G/c also requires v_G/c less power to operate, which is perhaps an even more important consideration for large-scale integration. Thus, for an electro-optic modulator or a switch, the device enhancement is a factor $(v_G/c)^2$. The same improvement by $(v_G/c)^2$ is achieved in an all-optical gate using the Kerr effect. In this case the δn change is self-induced by the signal itself, and δn is proportional to the local electric field squared. The savings in the length of the device is the same v_G/c as for an electro-optic device. In addition, because of the small v_G, the energy of the pulse is temporally compressed by a factor of v_G/c, so that the induced δn is $1/(v_G/c)$ times larger. Thus, for a pulse of a fixed total energy, we can actually use a device that is smaller by a factor of $\sim(v_G/c)^2$.

IMPROVEMENTS OFFERED BY PHOTONIC CRYSTALS

Photonic crystals (PC's) are ideal systems in which one can achieve arbitrarily low group velocities [9,10,11]. They are artificially created materials in which the index of refraction has a 1D, 2D, or 3D periodicity. Under appropriate conditions, and when the maximum index contrast is sufficiently large, a photonic band-gap appears: a range of frequencies in which light cannot propagate in the crystal. Because of this, photons inside a PC have many properties similar to electrons in semiconductors. Consequently, PCs are considered to be a promising media for large-scale integrated optics. In particular, line defects in a PC can lead to guided mode bands inside the photonic band gap. These bands can in principle be made as flat as desired by the appropriate design. Typical group velocities for reasonable linear-defect guided modes can easily be $\mathcal{O}(10^{-2}c\text{-}10^{-3}c)$, thus making it possible to shrink the size of all-optical and electro-optical devices in PC's by $\sim(v_G/c)^2\sim10^{-4}\text{-}10^{-6}$, while keeping the operating power *fixed*.

For definiteness, we focus our attention on a particular class of PC line-defect systems that can have very low group velocities; namely, we discuss Coupled Cavity Waveguides (CCW) [12,13]. A CCW consists of many cavities, as in Figure 2. Each of these cavities when isolated supports a resonant mode with the resonant frequency well inside the band-gap. When we bring such cavities close to each other, to form a linear defect as in Figure 2, the photons can propagate down the defect by tunneling from one cavity to another. Consequently, the group velocity is small, and the less closely coupled the cavities are, the slower the group velocity. Group velocities of c/1000 or even smaller are easy to attain in such systems.

Since the cavities in a CCW are so weakly coupled to each other, the tight-binding method [12,13,14,15] is an excellent approximation in deriving the dispersion relation. The result is: $\omega(k)=\Omega[1-\Delta\alpha+\kappa\cos(k\Lambda)]$, where Ω is the single-cavity resonant frequency, Λ is the physical distance between the cavities, and $\Delta\alpha\ll\kappa\ll1$ in the tight binding approximation, so we can approximate $\Delta\alpha=0$ in our analysis.

The CCW system has a zero-dispersion point at $k=\pi/2\Lambda$. We choose this to be the operation point of our devices, since the devices in that case have far larger bandwidths than most other slow-light systems would have; in our simulations, the useful bandwidth[†] of such CCW devices is typically more than 1/3 of the entire CCW band. To see that the CCW system is optimal with respect to bandwidth, we note that in order to maximize the bandwidth, one wants $\Delta k\equiv k(\omega,n+\delta n)-k(\omega,n)$ to be as independent of ω as possible, for as large a range of ω's as possible. One way to satisfy this is, for example, if $k(\omega)$ is nearly linear, and if the dominant effect of δn is to shift $k(\omega)$ upwards or downwards by a nearly constant amount. This is precisely what happens in CCW systems. First, note that $\omega(k,\delta n)=\Omega(1+\delta_1)[1+\kappa(1+\delta_2)\cos(k\Lambda)]$, where δ_1 and δ_2 are first order in δn. Thus, δn shifts the curve upwards by $\Omega\delta_1$, and also changes the slope at the zero-dispersion point: $\kappa\rightarrow\kappa(1+\delta_1)(1+\delta_2)$. But, since the slope was so small to start with (since $\kappa\ll1$ in slow-light systems), the dominant effect in $\Delta k(\omega,\delta n)$ is the linear shift upwards, which produces a term independent of ω.

To make the claim from the previous paragraph more precise, we can expand $\omega(k,\delta n)$ around the zero dispersion point, and invert the relation to get $k(\omega,\delta n)$, and thereby $\Delta k(\omega,\delta n)\approx[\delta_1\omega/\Omega+\delta_2(\omega/\Omega-1)]/\Lambda\kappa$. Moreover, since we are working with a slow-light band, we are interested only in ω's that can be written as $\omega=\Omega+\delta\omega$, where $\delta\omega\ll\Omega$. Thus $\Delta k(\delta\omega,\delta n)\approx[\delta_1+(\delta\omega/\Omega)*(\delta_1+\delta_2)]/\Lambda\kappa$, and since $\delta\omega/\Omega\ll1$, Δk is almost constant across most of the slow-light band. In fact, a similar derivation can easily be adapted to apply for any zero dispersion point of any flat dispersion curve. Consequently, if one wants to use slow light to enhance the non-linear phase sensitivity, one should operate at a zero-dispersion point because this optimizes the available bandwidth of the device, even in non-CCW systems.

SLOW-LIGHT PHOTONIC CRYSTAL MACH-ZEHNDER DEVICES

To demonstrate how the ideas above can be put to work in practice, we perform numerical simulation studies of a two-dimensional CCW system. The system is illustrated in Figure 2. It consists of a square lattice of high-ε dielectric rods ($\varepsilon_H=12.25$) embedded in a low-ε dielectric material ($\varepsilon_L=2.25$). The lattice spacing is denoted by a, and the radius of each rod is r=0.25a. The CCW is created by reducing the radius of each fourth rod in a line to r/3, so $\Lambda=4a$. We focus our attention on transverse-magnetic (TM) modes, which have electric field parallel to the rods.

To begin our study of the modes of this system, we perform frequency-domain calculations using preconditioned conjugate gradient minimization of the Rayleigh quotient in a 2D plane-wave basis as described in detail in Ref. 16. To model our system, we employ a supercell geometry of size (11a*4a) and a grid of 72 points per a. The results reveal an 18% photonic band-gap between $\omega_{MIN}=0.24(2\pi c)/a$ and $\omega_{MAX}=0.29(2\pi c)/a$. Adding a line defect of CCW's mutually spaced Λ apart, leads to a CCW band that can be excellently approximated by $\omega=[0.26522-0.00277\cos(k\Lambda)](2\pi c/a)$. This gives $v_G=0.0695c$ at the point of zero dispersion for the case $\Lambda=4a$. (To demonstrate our ideas, we use a v_G that is not extraordinarily small in

[†] For example, in a Mach-Zehnder interferometer, useful bandwidth would be defined as the range of ω's in which the extinction ratio >99% when the device is in its "off" state.

order to be less demanding on the time-domain numerical simulations.) The frequency-domain calculation further tells us that roughly 50% of energy of each mode is in the high-ε regions, and that this ratio is fairly independent of k.

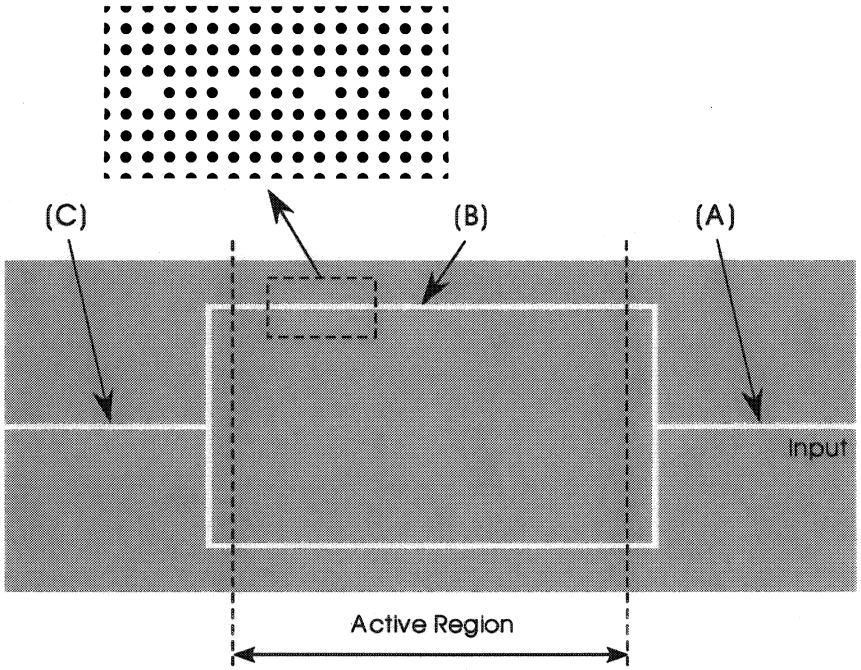

Figure 2: Sketch of a Mach-Zehnder interferometer that we use to demonstrate enhancement of non-linear phase sensitivity due to slow-light in photonic crystals. The slow-light system that we use is a Coupled Cavity Waveguide, as shown in the upper-left inset of this figure. (Throughout the article, cavities are white to make them more visible). The signal enters the device on the right, is split equally at the first T-branch into the upper and lower waveguides, and recombined at the T-branch on the left. If no index change is induced, the parts of the signal coming from the top and the bottom interfere constructively at the second T-branch, and the pulse exists entirely at the output. If we induce the index change in the active region in an appropriate manner, the two parts of the signal interfere destructively, and the pulse is reflected back towards the input, with no signal being observed at the output. The points marked (A),(B), and (C) correspond to field monitor points during the simulations. The results of observations from these points are displayed in Figure 3.

To put things in perspective, we can use the frequency-domain code results to estimate sizes of some real devices. For purposes of illustration only, we simulate a device in which we modify the high-ε material by $\delta n/n_H=2*10^{-3}$ to perform the switching, say through an electro-optical effect. We pick a somewhat unrealistically large $\delta n/n_H$ in order to lower the requirements on our numerical simulations; as mentioned earlier, the length of the system varies inversely with $\delta n/n_H$ and we can scale our results to experimentally realizable δn's accordingly. Let us now ask how long the CCW has to be in order for the signal to accumulate exactly π phase shift when propagating down this CCW, compared to the case when $\delta n=0$. We run the frequency domain code twice, using the two different values of ε_H, for 18 uniformly distributed k's between k=0, and k at the edge of the first Brillouin zone. Next, we perform the tight-binding curve-fits to the two sets of data. From these two fitted curves it is trivial to get Δk at the point of zero dispersion, and thereby L from the relation $L\Delta k=\pi$. The result is that the CCW has to be approximately $L=31.6\Lambda=35.5\lambda_{AIR}$ long to achieve a π phase shift when propagating down this CCW.

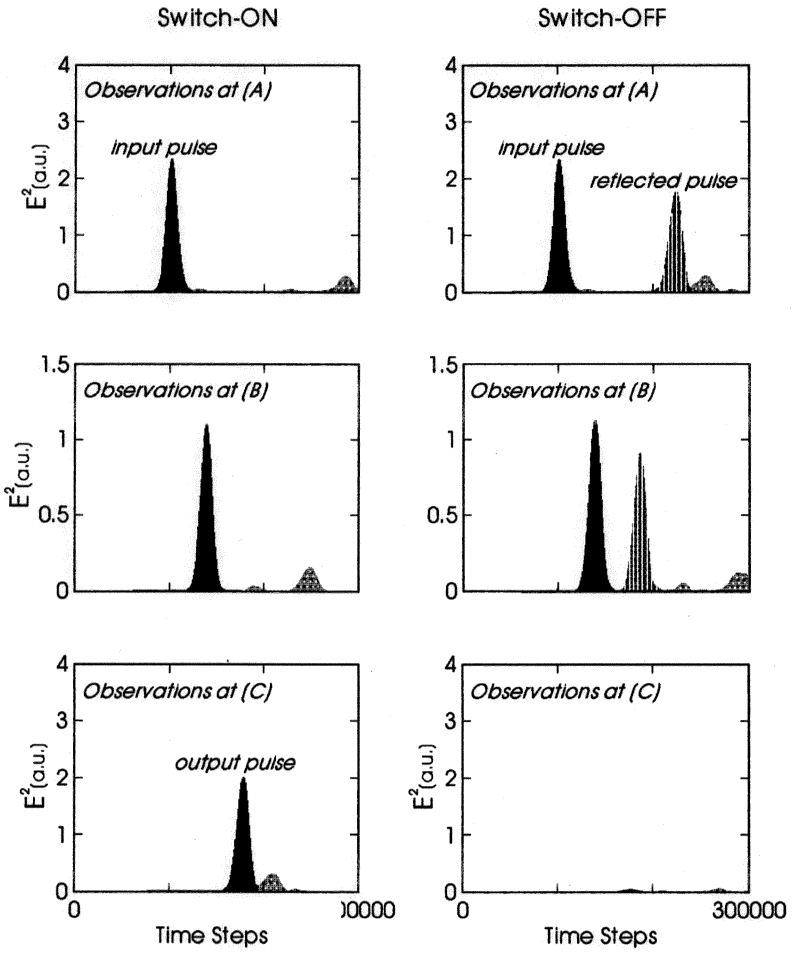

Figure 3: Demonstration of non-linear switching in a slow-light photonic crystal system. Electric field squared as a function of time, observed at three different points: (A),(B), and (C) in the system from Figure 2. The left column corresponds to the case when no index change is induced; most incoming signal (A) exits at the output (C). The column on the right corresponds to the case when the non-linear index change is induced; the signal at the output (C) in the right-hand column is drastically reduced compared to the output (C) in the left-hand column. The black and dashed-gray signals represent the pulses traveling from right-to-left, and left-to-right, respectively in Figure 2. The gray pulses are spurious reflections (mostly from the interface between the photonic crystal and air at the exits of the device.)

Based on what we learned from the frequency-domain calculations, we can now design a Mach-Zehnder interferometer for use in the time-domain. Specifically, we perform 2D finite-difference time-domain simulations [17], with perfectly-matched-layer (PML) absorbing boundary conditions [18]. Our numerical resolution is 24*24 points per a^2, meaning that the entire computational cell is 5000*696 points. Since our computational cell is large enough, we can easily distinguish the pulses reflected from the boundaries of our simulation, from the real physical pulses. For the waveguides, we use the CCWs as described earlier. The time-domain simulation reveals that there is a slow-light band between $\omega_{MIN}=0.2620(2\pi c)/a$ and $\omega_{MAX}=0.2676(2\pi c)/a$, which is within 0.2% of the frequency-domain prediction. Next, we use results of previous research to implement the needed 90° bends [19], and T branches [20]. At the input of our Mach-Zehnder interferometer, we launch a pulse with a Gaussian frequency profile, with carrier frequency of $\omega_0=0.2648(2\pi c)/a$ and FWHM $\Delta\omega/\omega_0=1/200$. During the simulations, we monitor the electric field, E(t), at 8 points in the system. We show the placement of 3 of these points in Figure 2. The observations at the other 5 points (which include the branch points and the end points) provide us with no new information, but are

monitored just to ensure self-consistency. When δn is off, as in the first column of Figure 3, the signal comes in at the input, splits equally into the two arms at the first branch, and recombines at the second branch, traveling towards the output, as seen in Figure 4. Apart from very small reflections (app. 2%) due to the lack of full, optimized branches, most of the signal reaches the output. Next we change the high-index material to $n_H \rightarrow (1+0.00166)n_H$ in the upper half of the active region in Figure 2, and $n_H \rightarrow (1-0.00166)n_H$ in the lower half of the active region in Figure 2[‡]. Because of this difference in n_H, the part of the signal traveling in the upper arm accumulates π more phase shift than the half traveling in the lower arm[§]. Thus, the signal interferes destructively at the output, and is reflected back towards the input, as seen in Figure 5. Even without any fine-tuning, we observe a signal at the output that is 16.4dB smaller than in the case when δn is not applied.

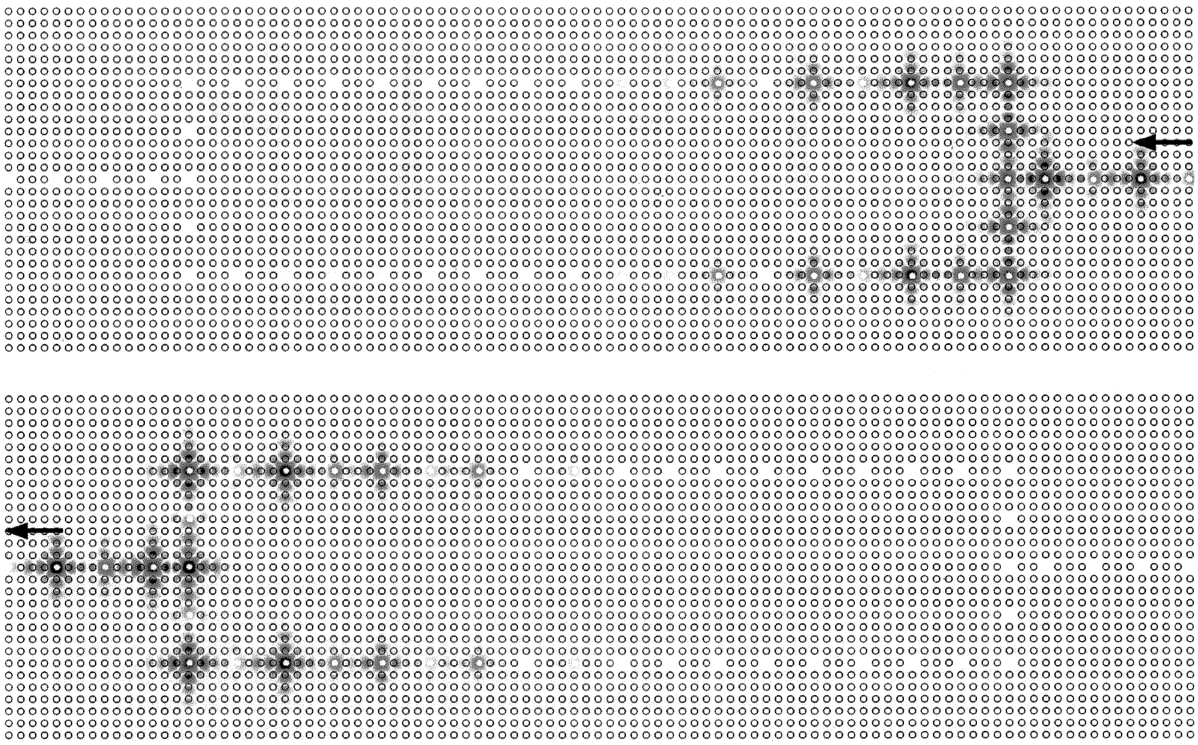

Figure 4: Snap-shots of electric field pulse in the system from Figure 2 for the case when no index change is induced. Top panel is at 120000 time steps, and bottom panel is at 160000 time steps. The signal entering at the input exits at the output of the device; the device is in its "on" state. (Throughout the article, cavities are white to make them more visible).

As mentioned before, CCWs have an added benefit in that the bandwidth of the device above is optimal due to the existence of the zero dispersion point. For example, the useful bandwidth of the device from Figures 2-5 is $\Delta\omega/\omega_0 \approx 1/150$. The useful bandwidth of the CCW devices scales roughly linearly with v_G/Λ for small δn. On the other hand, the performance gets better with $1/v_G^2$. Therefore, if we are willing to have a device with a smaller useful bandwidth, we can have a much more efficient device. For example, a

[‡] According to the frequency-domain prediction, the active region therefore needs to be approximately 16 coupled cavities long if $\delta n/n_H=0.002$; we find that we actually need $\delta n/n_H=0.00166$ in the time-domain calculation. We attribute most of the discrepancy to the inadequateness of the tight-binding approximation, finite bandwidth of the beam, and numerical inaccuracies of the simulations.

[§] One might wonder about the practicality of applying a large positive field in one arm and a large negative field in the other arm of such a tiny device. All that is required, however, is to establish a strong gradient of the field between the two arms.

40Gbit/s telecommunications stream has a bandwidth of $\Delta\omega/\omega_0 \approx 1/3000$, so we can afford to operate the device with pulses that have 400 times less energy than when using the device from Figures 2-5, for the same device size. An additional savings of power occurs in CCW systems because most of the power is tightly confined to the cavities. In contrast, in a uniform waveguide, power is uniformly distributed along it. This fact typically produces additional power savings of a factor of 2–3 or more, depending on the geometry of the system.

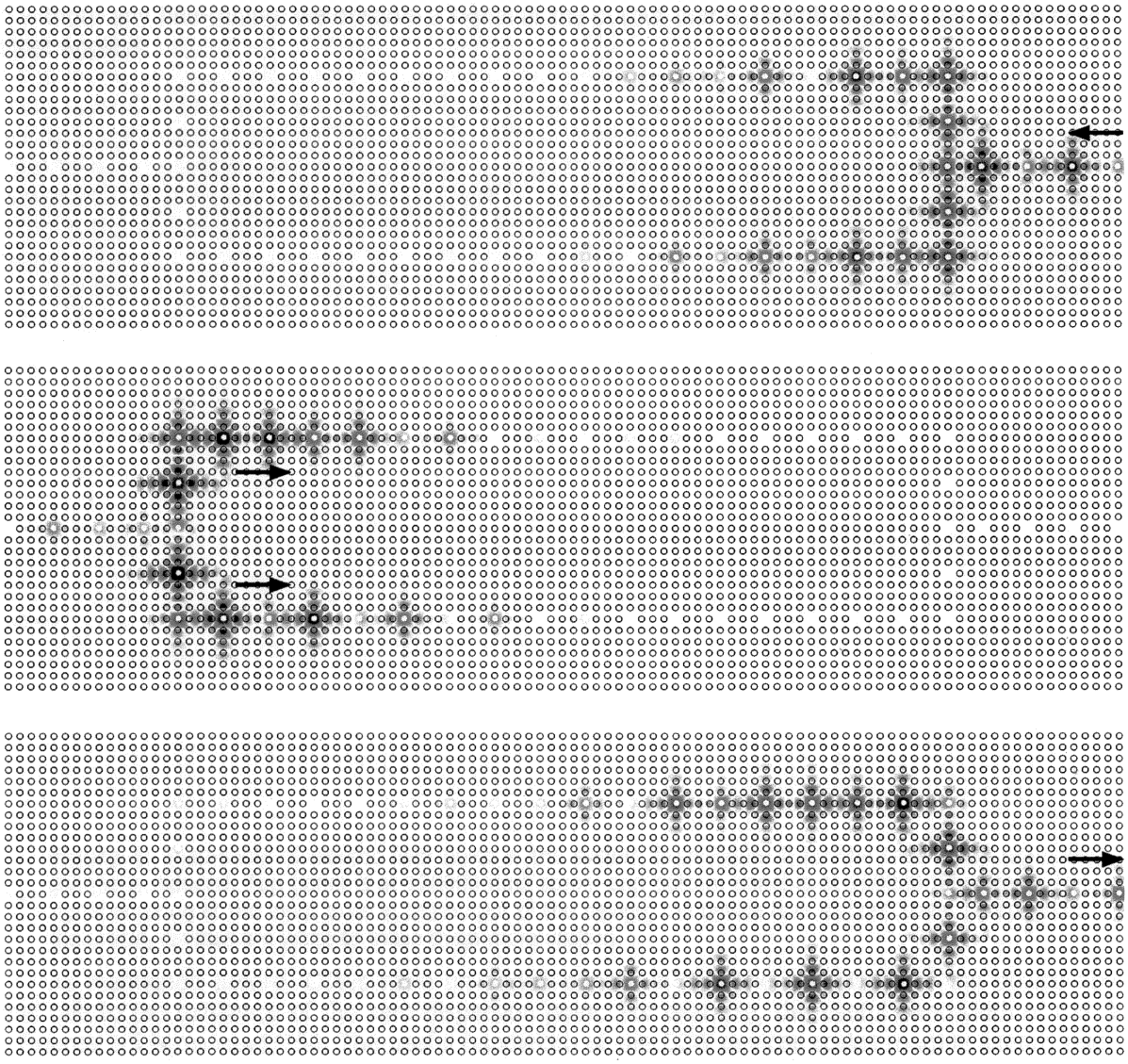

Figure 5: Snap-shots of electric field pulse in the system from Figure 2 for the case when an index change is induced. Top panel is at 120000 time steps, middle panel is at 160000 time steps, and bottom panel is at 200000 time steps. The signal entering at the input is reflected back towards the input; device is in its "off" state. (Throughout the article, cavities are white to make them more visible).

To make the idea of the previous paragraph a bit more explicit, we explore the possibility of an all-optical device with more optimized parameters. We envision a system like in Figures 2-5, but with coupled cavities spaced 6 lattice periods apart, so that Λ=6a. In this case, the group velocity is 0.022c (about a factor of 3 slower than in the case above). Now, we use the distribution of the fields given by the frequency-

domain code to calculate (using first order perturbation theory in the small quantity $\delta n(\mathbf{r})/n(\mathbf{r})$) what happens to the slow-light band once the non-linear Kerr effect is turned on. We apply the Kerr effect only in the high index regions, since high index materials typically have non-linear coefficients much higher than those of low index materials. We now pick physically realistic parameters so that the largest induced $\delta n/n$ anywhere is $2*10^{-4}$. In this case, the perturbation theory tells us that if we operate at the zero-dispersion point and the Kerr effect is present in only one arm of the interferometer, the length of the device has to be $70.97\Lambda=175\mu m$ at $\lambda=1.55\mu m$. The transverse size of the device would then be roughly $20\mu m$. Suppose that our high-index material has a Kerr coefficient $n_2=1.5*10^{-13}cm^2/W$ (which is a value achievable in a number of materials, GaAs at $\lambda_0=1.55\mu m$ being one of them), where the Kerr effect is given by $\delta n=n_2 I$. In that case, we would need roughly 0.26W peak power to operate our device. (For comparison, an integrated optics device made of same (uniform) high index material, with cross section area of $0.5\mu m*0.5\mu m$ would have to be 5cm long to operate at the same 0.26W peak power.) The useful bandwidth of our device would be at least $\Delta\omega/\omega_0\approx 1/670$, meaning that it could operate at bit rates greater than 100Gbit/s. For lower bit rates, with less bandwidth, the performance enhancements could be even greater. Finally, even the design outlined here can be further improved by confining more energy into high-ε regions, (for example, by using a triangular-lattice PC system with air holes in dielectric,) or by increasing the index contrast between the high-ε, and low-ε materials. By optimizing the design along these lines, one should be able to enhance the system by additional factors of 3-4 without much effort.

PHOTONIC CRYSTAL 1*2 SWITCH

The switching mechanism in this article is general enough for use in a variety of all-optical logical operations, switching, routing, wavelength conversion, optical imprinting, etc. For example, we can enhance the applicability of our design by allowing the device to have two outputs (like in the upper plot of Figure 6), instead of just one (like in Figure 2). In this case, the non-linear mechanism in question directs input to either of the two outputs. To achieve this, we put a directional coupler at the output of the device instead of terminating the device with a simple branch. The directional coupler has to be designed so that (depending on the relative phase of its two inputs) it directs both of them either to the upper, or the lower of its two outputs. Almost any directional coupler can be designed to perform this function.

A photonic crystal implementation could be based on the waveguide drop-filter design of Ref. 21. For this application, we need only to operate it at a frequency offset from that originally intended. An advantage of this particular design is that it adds only 1λ to the length of the entire device. The device of Ref. 21 involves two linear waveguides and a coupling element (consisting of two point-defect cavities) between them as shown in the inset of the upper panel of Figure 6. If we label the waveguides as "1" and "2", we can write:

$$A_{OUT1} = A_{IN1}\left(1-\frac{i\alpha}{\omega-\omega_0+i\alpha}\right)-A_{IN2}\left(\frac{i\alpha}{\omega-\omega_0+i\alpha}\right),$$

$$A_{OUT2} = A_{IN2}\left(1-\frac{i\alpha}{\omega-\omega_0+i\alpha}\right)-A_{IN1}\left(\frac{i\alpha}{\omega-\omega_0+i\alpha}\right), \qquad (2)$$

where A_{OUTj}, and A_{INj} are the amplitudes at the output and input of waveguide j, respectively, the central frequency of the two coupled cavities is ω_0, and 2α is the width of the resonance. In our device, we will have equal intensities coming to both inputs, and we would like all the energy to exit at a single output. If we look at this picture from a time-reversed perspective, this tells us that we have to operate the directional coupler at the frequency $\omega_0\pm\alpha$, rather than operating it at $\omega=\omega_0$, as is done in Ref. 21. This time-reversed picture also tells us that (according to Eqs.(2)) if we choose to operate at frequency $\omega_0+\alpha$, we get 100% transmission at the output of waveguide 2, if the input of waveguide 2 lags waveguide 1 in phase by exactly $\pi/2$. We get 100% transmission at the output of waveguide 1 if the input of waveguide 2 is $\pi/2$ ahead. The

dependence of transmission on the phase difference $\Delta\phi$ between waveguides 1 and 2 is illustrated in the lower plot of Figure 6. Operating at the frequency $\omega_0-\alpha$ reverses this relative-phase dependence.

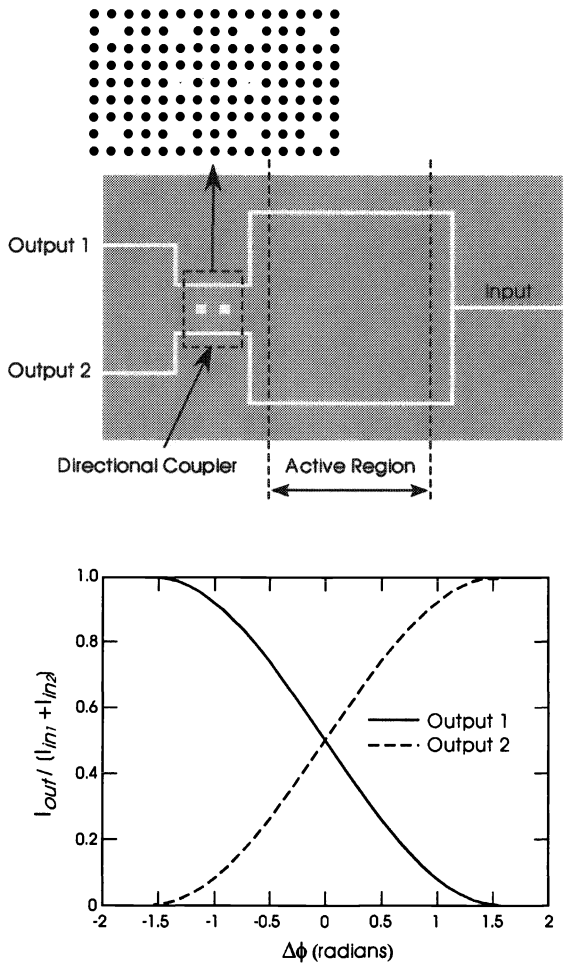

Figure 6: Mach-Zehnder interferometer operating as a router between two different outputs. This is achieved by terminating the interferometer with a directional coupler rather than with a T-branch, as shown in the upper panel. The lower panel gives the calculated intensity at each of the two outputs, as a function of the phase difference between the upper and the lower input to the directional coupler.

For example, let's pick as the operating frequency $\omega_0+\alpha$, and let's say that the intensities entering the device from the two waveguides are the same apart for the fact that waveguide 2 lags waveguide 1 in phase by $\pi/2$. Then:

$$\frac{I_{OUT1}}{I_{IN1}+I_{IN2}}=\frac{1}{2}\frac{(\omega-\omega_0-\alpha)^2}{(\omega-\omega_0)^2+\alpha^2},$$

$$\frac{I_{OUT2}}{I_{IN1}+I_{IN2}}=\frac{1}{2}\frac{(\omega-\omega_0+\alpha)^2}{(\omega-\omega_0)^2+\alpha^2}, \qquad (3)$$

where $I_{IN1,IN2}$ and $I_{OUT1,OUT2}$ denote the intensities at the inputs and outputs of the respective waveguides. According to Eqs.(3), the useful bandwidth of this directional coupler approximately equals 2α. In contrast to Ref. 21, we are not forced to operate in the regime of very small α; consequently, 2α can be readily

designed to be larger than the bandwidth of our Mach-Zehnder interferometer, so the directional coupler will not impair the performance of the device.

CONCLUDING REMARKS

The sizes of the non-linear devices described in this article using physically realistic values of δn are small enough to have 10^5 of them on a chip of surface size 2cm*2cm, operated at moderate pulse energy levels, and with speeds greater than 100Gbit/sec. Therefore, we view the work described here as an important step towards enabling large-scale integration of truly all-optical logic circuits. Finally, it should be emphasized that all of the results and arguments presented in this paper (which has focused on simplified 2D models) apply immediately to three dimensions. In fact, very recently, new 3D photonic crystal structures have been introduced that reproduce the properties of linear and point defect modes in 2D photonic crystal systems [22,23]. Such 3D structures should prove ideal candidates for eventual practical realization of the non-linear slow-light designs discussed in this work.

This work was supported in part by the Materials Research Science and Engineering Center program of the National Science Foundation under Grant No. DMR-9400334.

REFERENCES

1. W.E.Martin: "A new waveguide switch/modulator for integrated optics" Appl. Phys. Lett. **26**, 562-564 (1975).
2. Kawano, K.; Sekine, S.; Takeuchi, H.; Wada, M.; Kohtoku, M.; Yoshimoto, N.; Ito, T.; Yanagibashi, M.; Kondo, S.; Noguchi, Y.: "4*4 InGaAlAs/InAlAs MQW directional coupler waveguide switch modules integrated with spot-size converters and their 10 Gbit/s operation" Electronics Lett. **31**, 96-97 (1995).
3. A.Sneh, J.E.Zucker, and B.I.Miller: "Compact, low-crosstalk, and low-propagation-loss quantum-well Y-branch switches" IEEE Phot. Tech. Lett. **8**, 1644-1646 (1996).
4. Marin Soljačić, Steven G. Johnson, Shanhui Fan, Mihai Ibanescu, Erich Ippen, and J.D. Joannopoulos: "Photonic Crystal Slow-Light Enhancement of Non-linear Phase Sensitivity", an invited paper in the special issue of JOSA B devoted to Non-linear Photonic Crystals (to appear Sept. 2002).
5. S.E.Harris: "Electromagnetically Induced Transparency", Physics Today **50**, 36-42 (1997).
6. L.V.Hau, S.E.Harris, Z.Dutton, and C.H.Behroozi: "Light speed reduction to 17 metres per second in an ultracold atomic gas" Nature **397**, 594-598 (1999).
7. M.O.Scully, M.S.Zubairy, *Quantum Optics* (Cambridge University Press, Cambridge, 1997).
8. M.D.Lukin, and A.Imamoglu: "Controlling photons using electromagnetically induced transparency" Nature **413**, 273-276 (2001).
9. E. Yablonovitch: "Inhibited Spontaneous Emission in Solid-State Physics and Electronics", Phys. Rev. Lett. **58**, 2059-2062 (1987).
10. Sajeev John: "Strong localization of photons in certain disordered dielectric superlattices", Phys. Rev. Lett. **58**, 2486-2489 (1987).
11. J.D.Joannopoulos, R.D.Meade, and J.N.Winn, *Photonic Crystals: Molding the flow of light* (Princeton University Press, Princeton, N.J., 1995).
12. A.Yariv, Y.Xu, R.K.Lee, and A. Scherer: "Coupled-resonator opticalwaveguide:a proposal and analysis" Opt. Lett. **24**, 711-713 (1999).

13. M.Bayindir, B.Temelkuran, and E.Ozbay: "Tight-Binding Description of the Coupled Defect Modes in Three-Dimensional Photonic Crystals", Phys. Rev. Lett. **84**, 2140-2143 (2000).

14. See, for example, N.W.Ashcroft, and N.D.Mermin, *Solid State Physics* (Saunders, Philadelphia, PA, 1976).

15. E. Lidorikis, M. M. Sigalas, E. N. Economou, and C. M. Soukoulis: "Tight-Binding Parametrization for Photonic Band Gap Materials", Phys. Rev. Lett. **81**, 1405-1408 (1998).

16. Steven G. Johnson and J. D. Joannopoulos: "Block-iterative frequency-domain methods for Maxwell's equations in a planewave basis" Optics Express **8**, no. 3, 173-190 (2001).

17. For a review, see A.Taflove, Computational Electrodynamics: The Finite-Difference Time-Domain Method (Artech House, Norwood, Mass., 1995).

18. J.P.Berenger: "A perfectly matched layer for the absorption of electromagnetic waves", Journal of Computational Physics, **114**, 185-200 (1994).

19. A.Mekis, J.C.Chen, I.Kurland, S.Fan, P.R.Villeneuve, and J.D.Joannopoulos: "High Transmission through Sharp Bends in Photonic Crystal Waveguides", Phys. Rev. Lett. **77**, 3787-3790 (1996).

20. S.Fan, S.G.Johnson, J.D.Joannopoulos, C.Manolatou, and H.A.Haus: "Waveguide branches in photonic crystals" J. Opt. Soc. Am. B, **18**, 162-165 (2001).

21. Shanhui Fan, Pierre R.Villeneuve, J.D.Joannopoulos, and H.A. Haus: "Channel Drop Tunneling through Localized States", Phys. Rev. Lett. **80**, 960-963 (1998).

22. S.G.Johnson, and J.D.Joannopoulos: "Three-dimensionally periodic dielectric layered structure with omnidirectional photonic band gap" Appl. Phys. Lett. **77**, 3490-3492 (2000).

23. M.L.Povinelli, S.G.Johnson, S.Fan, and J.D.Joannopoulos: "Emulation of two-dimensional photonic crystal defect modes in a photonic crystal with a three-dimensional photonic band gap" Phys. Rev. B **64**, 075313(1-8) (2001).